Effects of DNA end configuration on XRCC4-DNA ligase IV and its stimulation of Artemis activity

Received for publication, May 26, 2017, and in revised form, July 5, 2017 Published, Papers in Press, July 10, 2017, DOI 10.1074/jbc.M117.798850

Christina A. Gerodimos, Howard H. Y. Chang, Go Watanabe, and Michael R. Lieber[1]

From the Departments of Pathology, Biochemistry & Molecular Biology, and Molecular Microbiology & Immunology and the Department of Biological Sciences, Section of Molecular & Computational Biology, Norris Comprehensive Cancer Center, University of Southern California Keck School of Medicine, Los Angeles, California 90033

Edited by Patrick Sung

In humans, nonhomologous DNA end-joining (NHEJ) is the major pathway by which DNA double-strand breaks are repaired. Recognition of each broken DNA end by the DNA repair protein Ku is the first step in NHEJ, followed by the iterative binding of nucleases, DNA polymerases, and the XRCC4-DNA ligase IV (X4-LIV) complex in an order influenced by the configuration of the two DNA ends at the break site. The endonuclease Artemis improves joining efficiency by functioning in a complex with DNA-dependent protein kinase, catalytic subunit (DNA-PKcs) that carries out endonucleolytic cleavage of 5′ and 3′ overhangs. Previously, we observed that X4-LIV alone can stimulate Artemis activity on 3′ overhangs, but this DNA-PKcs-independent endonuclease activity of Artemis awaited confirmation. Here, using *in vitro* nuclease and ligation assays, we find that stimulation of Artemis nuclease activity by X4-LIV and the efficiency of blunt-end ligation are determined by structural configurations at the DNA end. Specifically, X4-LIV stimulated Artemis to cut near the end of 3′ overhangs without the involvement of other NHEJ proteins. Of note, this ligase complex is not able to stimulate Artemis activity at hairpins or at 5′ overhangs. We also found that X4-LIV and DNA-PKcs interfere with one another with respect to stimulating Artemis activity at 3′ overhangs, favoring the view that these NHEJ proteins are sequentially rather than concurrently recruited to DNA ends. These data suggest specific functional and positional relationships among these components that explain genetic and molecular features of NHEJ and V(D)J recombination within cells.

DNA double-strand breaks (DSBs)[2] are common events in multicellular eukaryotes, occurring at a rate of ~10 DSBs/cell/day (1–3). These breaks can arise physiologically, generated by recombination activating gene (RAG) proteins in V(D)J recombination, or pathologically, from causes including ionizing radiation, oxygen free radicals, and inadvertent enzymatic action (1, 4–8). In diploid yeast, DSBs are resolved through homologous recombination, which takes place during late S and G_2 phases when a homology donor can be used for homology-directed repair. Nonhomologous DNA end-joining (NHEJ) does not depend on the presence of a homology partner and occurs throughout the cell cycle, making it the predominant pathway utilized for repair of DSBs in vertebrate somatic cells (9, 10).

NHEJ is initiated when Ku, a heterodimer of Ku70 and Ku80, is recruited to the site of a DSB, allowing for subsequent recruitment of the Artemis endonuclease; DNA-dependent protein kinase, catalytic subunit (DNA-PKcs); the X-ray repair cross-complementing protein 4 (XRCC4)-DNA ligase IV complex (X4-LIV); DNA polymerases μ and λ; and accessory factors XRCC4-like factor (XLF)/Cernunnos and paralog of XRCC4 and XLF (PAXX), as needed (11, 12). The flexibility of the NHEJ pathway is reflected in the capacity of core factors to act iteratively and in any order on a variety of structurally and chemically diverse DNA ends, contingent upon which steps are necessary for a break to be resolved (13).

Artemis is the only nuclease required for NHEJ, although other nucleases (*e.g.* PNK-APTX-like factor (PALF or APLF)) may be involved (14). Alone, Artemis can act as a 5′ exonuclease (15). Artemis complexed with autophosphorylated DNA-PKcs has endonuclease activity and hairpin opening activity (16–18). Recent evidence indicates that NHEJ-mediated repair of DSBs is dependent upon the DNA end structural configuration (19). Importantly, the Artemis·DNA-PKcs nuclease and X4-LIV are sufficient for processing and ligation of overhangs with short regions (≤4 nt) of internal microhomology (19). It was observed, however, that X4-LIV and Artemis, without DNA-PKcs, generates both cleavage and ligation products using DNA with 3′ overhang ends; the addition of Ku does not affect this activity. Further testing confirmed that this was not a result of transient annealing between two DNA substrates, but a DNA-PKcs-independent nuclease activity of Artemis that occurs in the absence of another DNA end (19).

Here, we investigate the mechanism by which Artemis acts as an endonuclease on dsDNA without DNA-PKcs through the involvement of X4-LIV. We find that Artemis is recruited by X4-LIV to specific DNA end structural configurations, namely a protruding 3′-OH at an overhang, where the interaction of X4-LIV with Artemis permits nucleolytic action. We also discuss

This work was supported, in whole or in part, by National Institutes of Health grants (to M. R. L.). The authors declare that they have no conflicts of interest with the contents of this article. The content is solely the responsibility of the authors and does not necessarily represent the official views of the National Institutes of Health.

This article contains supplemental Fig. S1.

[1] To whom correspondence should be addressed. Tel.: 323-865-0568; E-mail: lieber@usc.edu.

[2] The abbreviations used are: DSB, double-strand break; NHEJ, nonhomologous DNA end-joining; DNA-PKcs, DNA-dependent protein kinase, catalytic subunit; XRCC4, X-ray repair cross-complementing protein 4; X4-LIV, XRCC4-DNA ligase IV complex; nt, nucleotide(s); Ni-NTA, nickel-nitrilotriacetic acid.

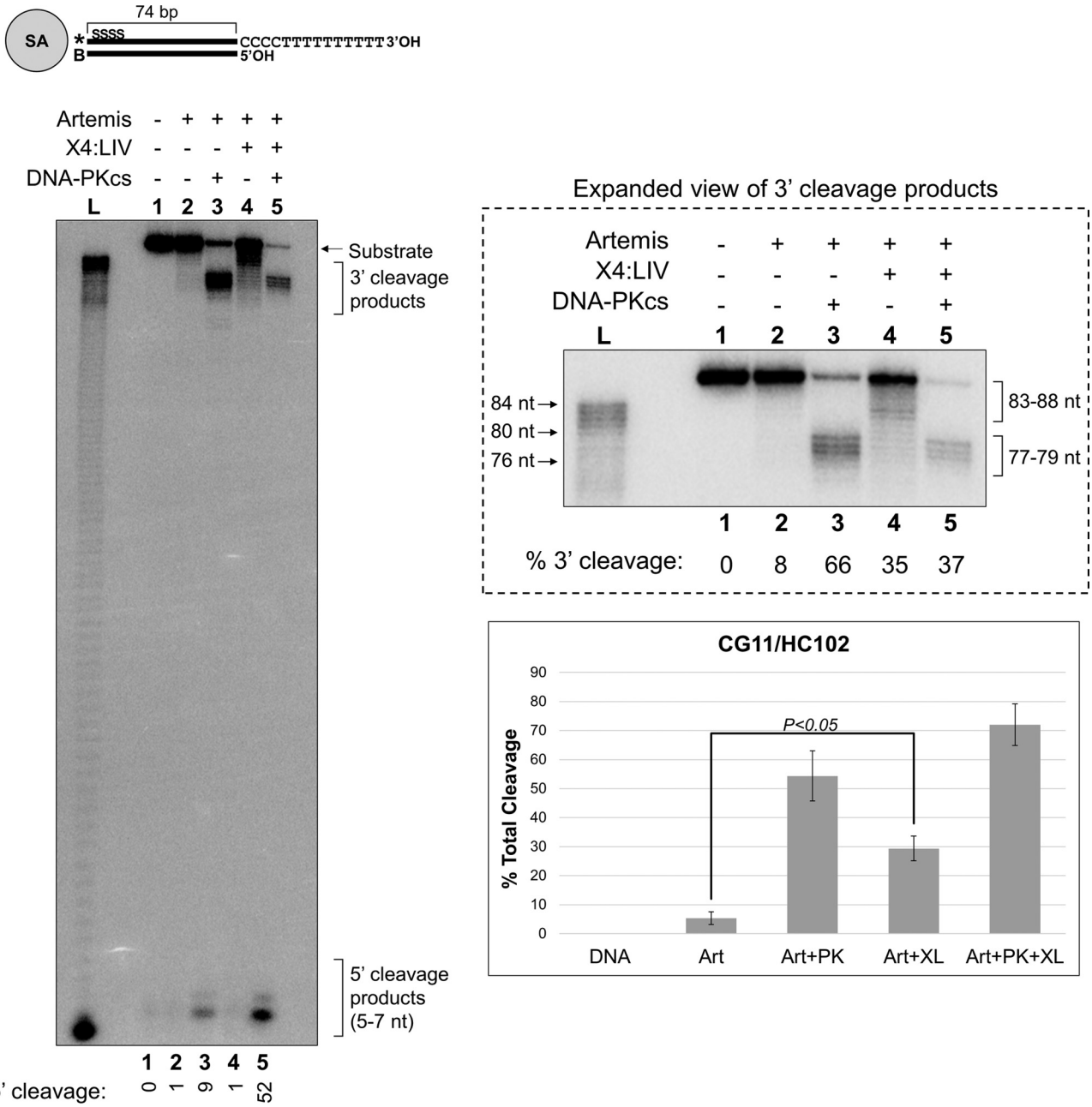

Figure 1. XRCC4-DNA ligase IV stimulates Artemis nuclease action on a 3′ overhang DNA end. 50 nM Artemis, 100 nM X4-LIV, and 25 nM DNA-PKcs were incubated with 40 nM *CG11/HC102 at 37 °C for 60 min. DNA was incubated with 200 nM streptavidin prior to the addition of NHEJ proteins to suppress protein binding or enzyme action at the biotinylated DNA end. Ladders (*lane L*) were generated by incubating 0.4 milliunits/ml of snake venom phosphodiesterase with 80 nM *CG12 at 37 °C for 10 min. DNA was resolved using 8% denaturing PAGE. The first 5 nt of the top strand contain phosphorothioate linkages. The *asterisk* indicates a ^{32}P radiolabel, *B* indicates biotin, and *SA* indicates streptavidin. Cleavage efficiency was calculated by dividing the signal of cleavage products by the total signal in each lane. Efficiency values were normalized to background signal in the substrate-only lane. This figure is representative of three gels from very similar experiments. The same basic result was observed in numerous additional experiments with other preparations of X4-LIV. Cleavage efficiency mean ± S.E. were calculated for each of five conditions (substrate only (DNA); Artemis (*Art*); Artemis and DNA-PKcs (*Art*+*PK*); Artemis and X4-LIV (*Art*+*XL*); and Artemis, DNA-PKcs, and X4-LIV (*Art*+*PK*+*XL*)). A Student's *t* test was used to determine *p* values for differences in cleavage efficiency between Art and Art + XL conditions, where $p < 0.05$ indicates significance. The graph represents the statistical analysis for the 3′ overhang substrate CG11/HC102, where $p = 0.02$.

how this DNA-PKcs-independent Artemis activity is compatible with the known genetics and molecular biology of NHEJ.

Results

XRCC4-DNA ligase IV stimulates Artemis endonuclease activity on 3′ overhangs without DNA-PKcs

Previously, we have observed that X4-LIV alone is capable of stimulating Artemis action on a 10-nt 3′ overhang (19). Artemis has intrinsic 5′ exonuclease activity on ssDNA, but requires activation by DNA-PKcs to endonucleolytically cleave 3′ ends (17). To confirm the DNA-PKcs-independent endonuclease activity, we incubated a radiolabeled 74-bp duplex DNA substrate containing a 14-nt 3′ overhang with Artemis alone, Artemis and DNA-PKcs, Artemis and X4-LIV, or all three (Fig. 1). To minimize cutting of transiently denatured DNA at the 5′ end of the top strand, phosphorothioate linkages were incorpo-

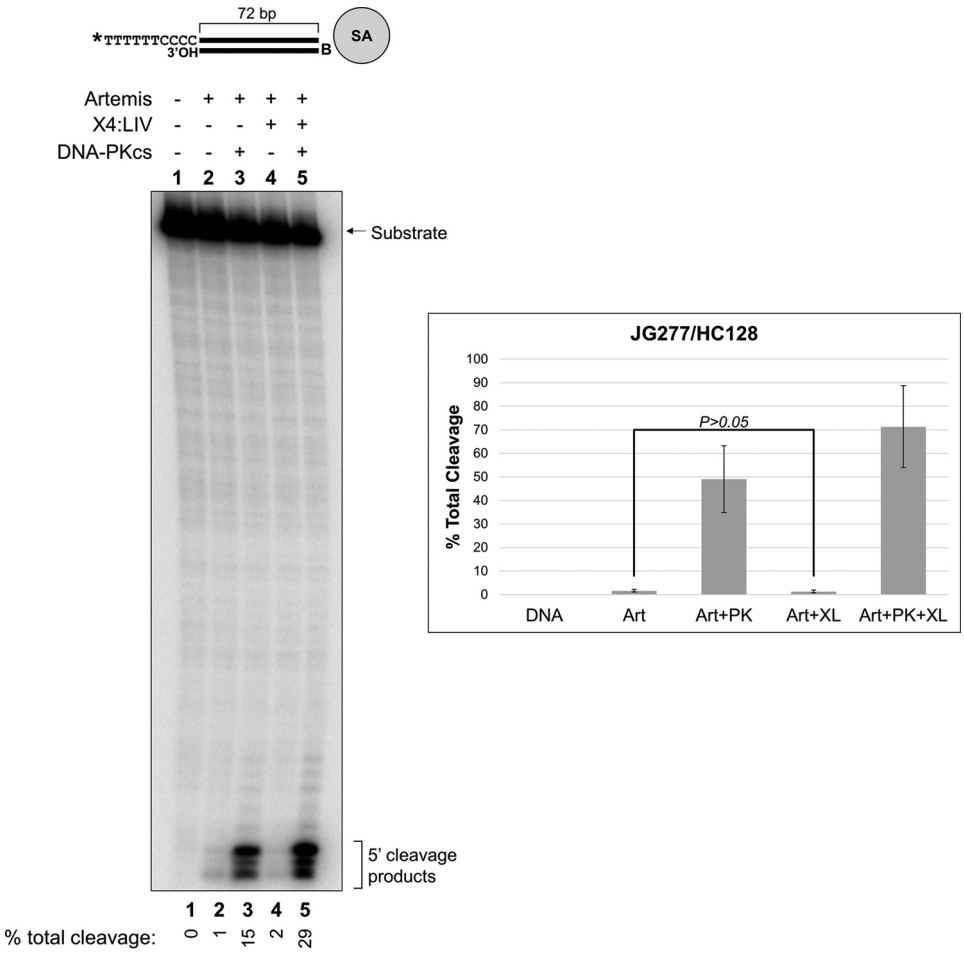

Figure 2. XRCC4-DNA ligase IV does not stimulate Artemis nuclease action on a 5′ overhang DNA end. 50 nM Artemis, 100 nM X4-LIV, and 25 nM DNA-PKcs were incubated with 40 nM *JG277/HC128 at 37 °C for 60 min. DNA was incubated with 200 nM streptavidin prior to the addition of NHEJ proteins to suppress protein binding or enzyme action at the biotinylated DNA end. DNA was resolved using 8% denaturing PAGE. The *asterisk* indicates a ^{32}P radiolabel, *B* indicates biotin, and *SA* indicates streptavidin. Cleavage efficiency was calculated by dividing the signal of cleavage products by the total signal in each lane. Efficiency values were normalized to background signal in the substrate-only lane. This figure is representative of three gels from very similar experiments. Statistical analysis was performed as previously described. The graph represents the statistical analysis for the 5′ overhang substrate JG277/HC128, where $p = 0.74$.

rated into the first 5 nt. Furthermore, 3′ biotinylation of the bottom strand was used to prevent action of Artemis at this same DNA end. (We have found that using streptavidin to suppress protein binding or enzyme action at biotinylated ends is not 100% effective and that the Artemis·DNA-PKcs complex can overcome this, as demonstrated in the present study by the generation of a low level of 5′ cleavage products.) As expected, we observe Artemis activity at the 3′ overhang in the presence of DNA-PKcs (Fig. 1, *lanes 3* and *5*). More importantly, we found that Artemis indeed cuts the 3′ overhang with a higher efficiency in the presence of X4-LIV than it does alone (Fig. 1, *lane 2 versus 4*). These data indicate that Artemis is stimulated by X4-LIV for endonuclease activity on a 3′ overhang in the absence of DNA-PKcs.

Artemis requires DNA-PKcs for cleavage of 5′ overhangs

We wondered if Artemis activity on 5′ overhangs would also be stimulated by X4-LIV alone (*i.e.* without DNA-PKcs). To test this, we incubated a radiolabeled 72-bp duplex DNA substrate containing a 10-nt 5′ overhang with proteins, as described (Fig. 2).

As expected, Artemis alone is not able to cleave the 5′ overhang (Fig. 2, *lane 2*). Artemis, in the presence of DNA-PKcs, acts on the 5′ overhang with a high efficiency, comparable with that observed for 3′ overhangs (Fig. 1, *lanes 3* and *5 versus* Fig. 2, *lanes 3* and *5*). However, the endonucleolytic cutting efficiency of Artemis in the presence of X4-LIV is not greater than that of Artemis alone (Fig. 2, *lane 2 versus 4*). These data show that Artemis activity on 3′ overhangs can be stimulated by X4-LIV, but is not stimulated for 5′ overhangs.

XRCC4-DNA ligase IV alone does not stimulate Artemis hairpin nicking activity

As Artemis and X4-LIV alone (*i.e.* without DNA-PKcs) cut at 3′ overhangs, but not at 5′ overhangs, we wondered if X4-LIV could stimulate Artemis hairpin nicking activity, which is required for opening DNA hairpins formed at coding ends during V(D)J recombination. To test this, we used a 20-bp blunt-ended hairpin substrate (Fig. 3). Artemis preferentially nicks 2 nt 3′ of the hairpin tip, where steric constraints on these base pairs result in the formation of a single-stranded/double-stranded DNA (ss/dsDNA) boundary (16). This activity gener-

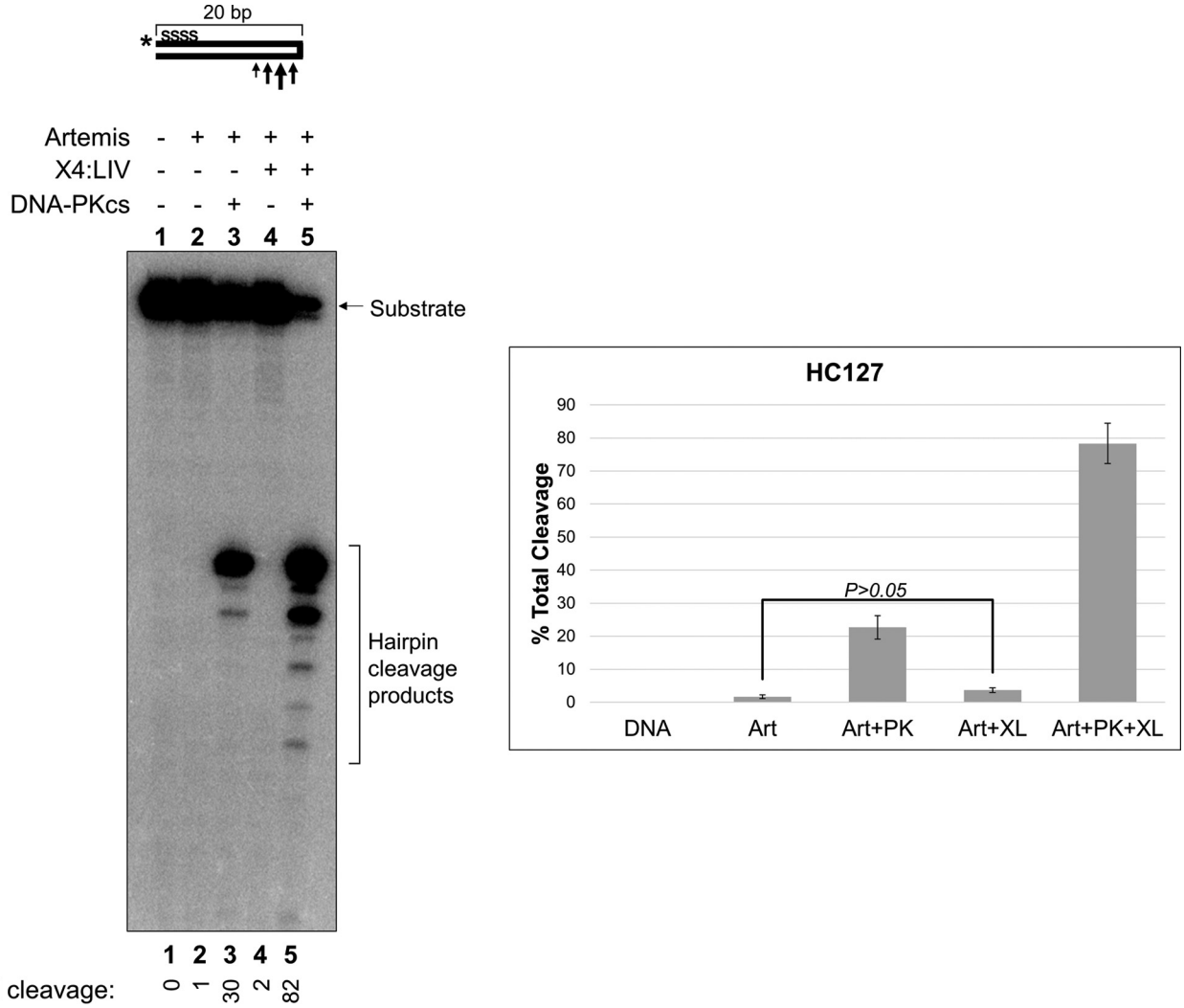

Figure 3. XRCC4-DNA ligase IV does not stimulate Artemis nuclease action on a DNA hairpin. 50 nM Artemis, 100 nM X4-LIV, and 25 nM DNA-PKcs were incubated with 40 nM *HC127 at 37 °C for 60 min. DNA was resolved using 12% denaturing PAGE. The first 5 nt of the substrate contain phosphorothioate linkages. The *asterisk* indicates a ^{32}P radiolabel. The *arrows* indicate major and minor cleavage sites for the generation of hairpin cleavage products, which are predominantly 21 to 23 nt from the radiolabel. Cleavage efficiency was calculated by dividing the signal of cleavage products by the total signal in each lane. Efficiency values were normalized to background signal in the substrate-only lane. This figure is representative of three gels from very similar experiments. Statistical analysis was performed as previously described. The graph represents the statistical analysis for the hairpin substrate HC127, where $p = 0.14$.

ates 4-nt 3′ overhangs that may be further processed for downstream ligation (16). We found that these nicked hairpin products are formed in the presence of DNA-PKcs, but not X4-LIV alone (Fig. 3, *lanes 3–5*).

Interestingly, although X4-LIV alone does not stimulate Artemis hairpin nicking activity, we found that the addition of X4-LIV to Artemis and DNA-PKcs results in an increase in hairpin nicking, as well as the generation of additional hairpin cleavage products (Fig. 3, *lane 3 versus 5*). This may be due to the formation of a 4-nt 3′ overhang upon hairpin nicking by the Artemis·DNA-PKcs complex, which allows for interaction of X4-LIV with the overhang via the terminal 3′-OH and, as a result, increased stimulation of Artemis activity at this end. These data show that X4-LIV does not stimulate Artemis activity on hairpins.

A 3′-OH at a 3′ overhang is required for XRCC4-DNA ligase IV stimulation of Artemis

Recognizing that X4-LIV alone stimulates Artemis at 3′ overhangs, but not at 5′ overhangs or hairpins, we wondered if an available 3′-hydroxyl group (3′-OH) is essential for this stimulation to occur. To test this, we used a 74-bp substrate similar to that used in our first test, but replaced the 3′ terminal deoxynucleotide in the overhang with a 2′, 3′-dideoxynucleotide.

We again observed that cutting of the 3′ overhang occurred when DNA-PKcs was present (Fig. 4, *lanes 3* and *5*). However, the cutting efficiency of Artemis and X4-LIV was not substantially greater than that of Artemis alone (Fig. 4, *lane 2 versus 4*). Fold-changes in cleavage efficiencies in reactions containing DNA-PKcs are comparable with those observed for the same reactions in our first experiment (Fig. 1, *lanes 3* and *5 versus* Fig. 4, *lanes 3* and *5*), indicating that Artemis cutting in the presence of X4-LIV alone can be attributed to an interaction between X4-LIV and the 3′-OH, and not a change in the enzymatic activity of Artemis.

To determine whether the recessed 5′-OH on the unlabeled bottom strand contributes to this DNA-PKcs-independent activity, we added a nonradioactive 5′-PO_4 here and found that

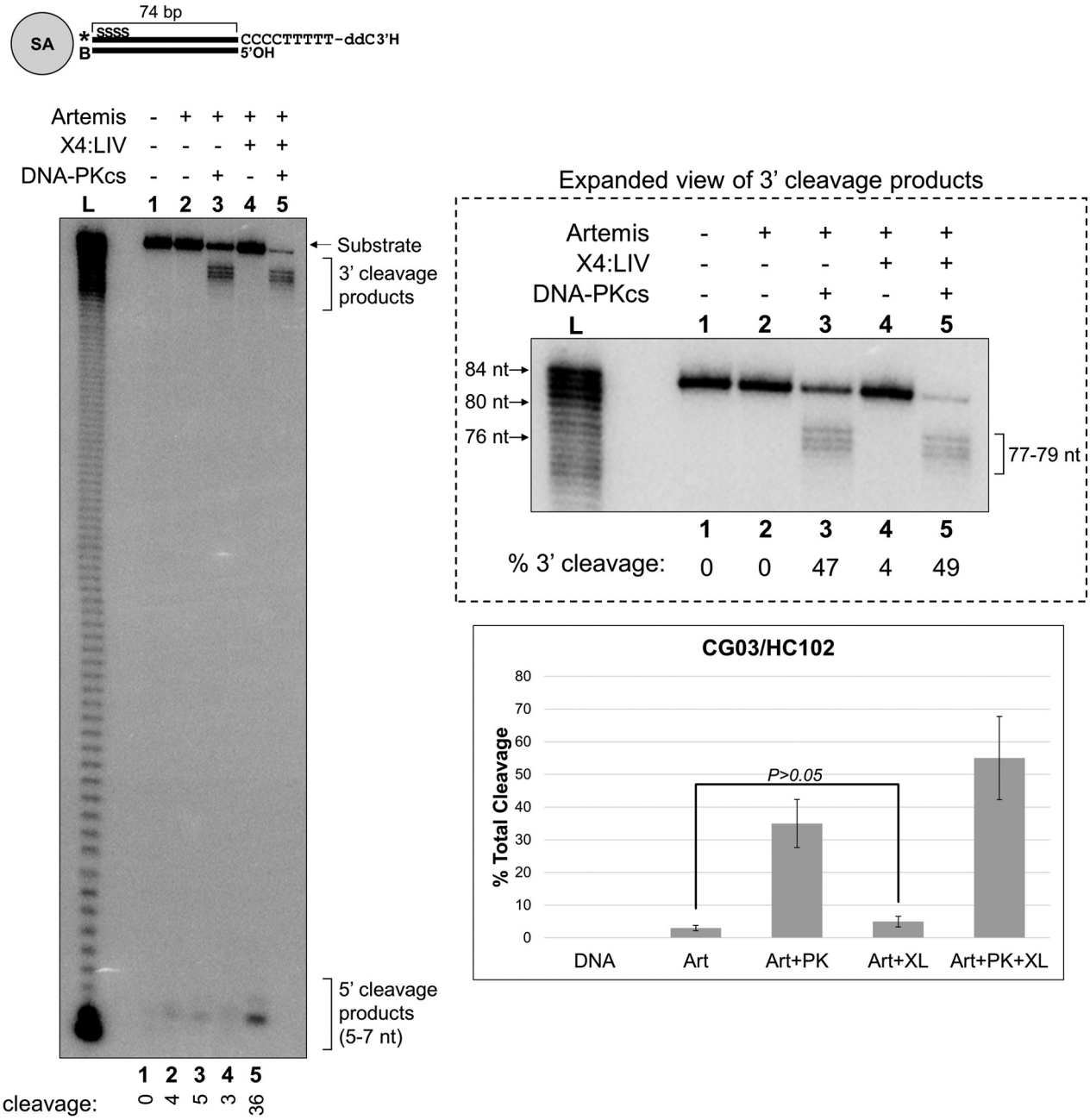

Figure 4. XRCC4-DNA ligase IV does not stimulate Artemis activity on a 3′ overhang DNA end lacking a terminal 3′-hydroxyl group. 50 nM Artemis, 100 nM X4-LIV, and 25 nM DNA-PKcs were incubated with 40 nM *CG03/HC102 at 37 °C for 60 min. DNA was incubated with 200 nM streptavidin prior to the addition of NHEJ proteins to suppress protein binding or enzyme action at the biotinylated DNA end. Ladders (*lane L*) were generated by incubating 0.4 milliunits/ml of snake venom phosphodiesterase with 80 nM *CG12 at 37 °C for 10 min. DNA was resolved using 8% denaturing PAGE. The first 5 nt of the top strand contain phosphorothioate linkages. The *asterisk* indicates a ^{32}P radiolabel, *B* indicates biotin, *SA* indicates streptavidin, and *ddC* indicates a 2′,3′-dideoxycytidine. Cleavage efficiency was calculated by dividing the signal of cleavage products by the total signal in each lane. Efficiency values were normalized to background signal in the substrate-only lane. This figure is representative of three gels from very similar experiments. Statistical analysis was performed as previously described. The graph represents the statistical analysis for the 3′ overhang substrate containing a 3′ terminal dideoxycytidine CG03/HC102, where $p = 0.42$.

X4-LIV stimulation of Artemis was unaffected by this feature of the DNA end (supplemental Fig. S1).

A 3′-OH but not a 5′-PO$_4$ at both DNA ends is critical for XRCC4-DNA ligase IV ligation activity

We wondered if certain chemical features of DNA ends were being utilized as recognition elements for X4-LIV, allowing it to bind these ends and then recruit Artemis for endonucleolytic action. If so, we posited that the addition or removal of X4-LIV recognition elements would affect the rate of ligation independent of Artemis or DNA-PKcs. Recent evidence shows that DNA end chemistry, particularly a 5′-PO$_4$, indeed acts as a recognition element for X4-LIV, serving to stabilize bridging of broken DNA ends (20).

We have found that nuclease activity by Artemis is required for efficient ligation of non-complementary DNA overhang

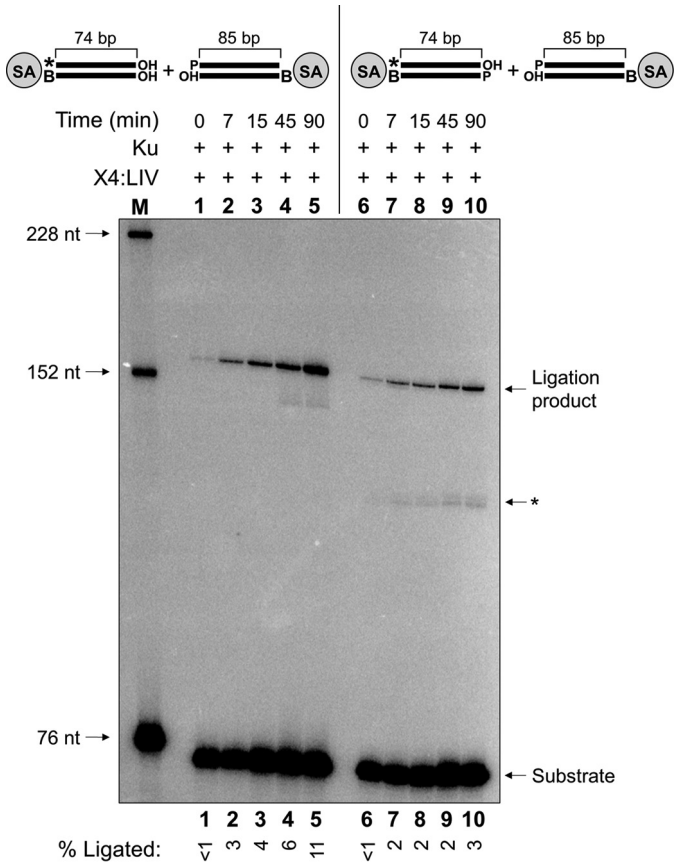

Figure 5. A second 5′ phosphate group is not essential for ligation of two blunt DNA ends. 50 nM Ku and 100 nM X4-LIV were incubated with 20 nM radiolabeled duplex DNA (*HC121/HC102 or *HC121/pHC102) and 20 nM pHC115/HC120 at 37 °C for 90 min, and ligation efficiency was measured at the specified time points. DNA was incubated with 200 nM streptavidin prior to the addition of NHEJ proteins to suppress protein binding or enzyme action at the biotinylated DNA ends. Markers (*lane M*) were generated by incubating *JG163/JG166 for 60 min under the same conditions. DNA was resolved using 8% denaturing PAGE. The first 5 nt of the radiolabeled top strand contain phosophorothioate linkages. The *asterisk* indicates a ^{32}P radiolabel, *B* indicates biotin, *SA* indicates streptavidin, *P* indicates a 5′-phosphate group, and *OH* indicates a 3′- or 5′-hydroxyl group. Two bands denoted by an *asterisk* are a result of self-dimerization and hairpinning of the radiolabeled duplex in a "head-to-head" or "tail-to-tail" orientation. Ligation efficiency was calculated by dividing the signal of ligation products by the total signal in each lane. This figure is representative of three gels from very similar experiments.

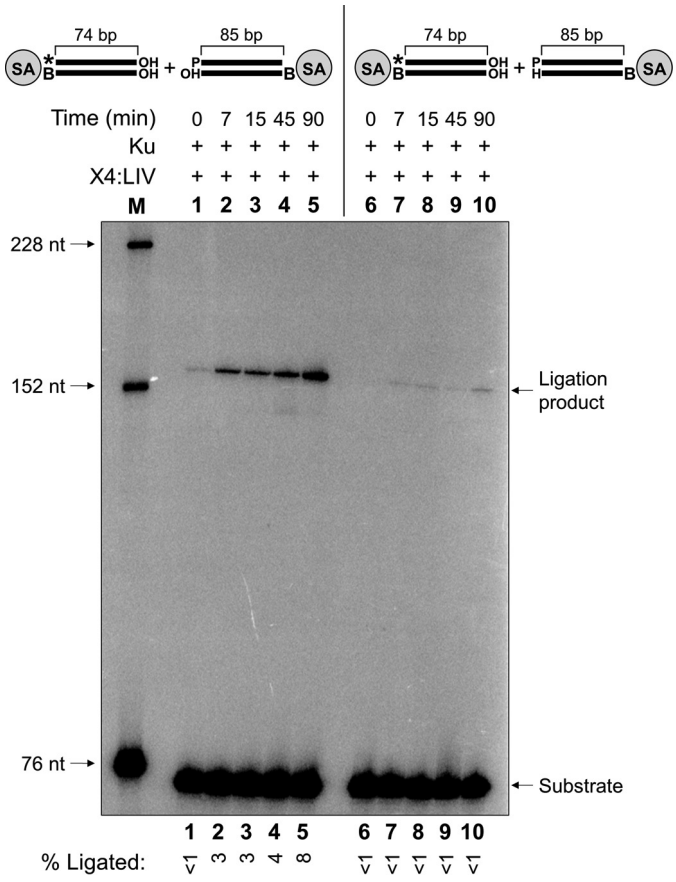

Figure 6. Two 3′-hydroxyl groups are required for ligation of two blunt DNA ends. 50 nM Ku and 100 nM X4-LIV were incubated with 20 nM *HC121/HC102 and 20 nM unlabeled duplex DNA (pHC115/HC120 or pHC115/CG04) at 37 °C for 90 min, and ligation efficiency was measured at the specified time points. DNA was incubated with 200 nM streptavidin prior to the addition of NHEJ proteins to suppress protein binding or enzyme action at the biotinylated DNA ends. Markers (*lane M*) were generated by incubating *JG163/JG166 for 60 min under the same conditions. DNA was resolved using 8% denaturing PAGE. The first 5 nt of the radiolabeled top strand contain phosphorothioate linkages. The *asterisk* indicates a ^{32}P radiolabel, *B* indicates biotin, *SA* indicates streptavidin, *P* indicates a 5′-phosphate group, *OH* indicates a 3′- or a 5′-hydroxyl group, and *H* indicates a 3′ hydrogen. Ligation efficiency was calculated by dividing the signal of ligation products by the total signal in each lane. This figure is representative of three gels from very similar experiments.

ends, whereas only Ku and X4-LIV are required for efficient ligation of blunt ends (19). To test the effect of the 5′-PO_4 on ligation of DNA ends independent of Artemis, we incubated a blunt-ended DNA duplex containing a 5′-PO_4 on the top strand with either of two radiolabeled blunt-ended duplexes, one of which contains a 5′-OH on the bottom strand (Fig. 5, *lanes 1–5*) and the other a 5′-PO_4 at this site (Fig. 5, *lanes 6–10*). The "outside" DNA end of each duplex was biotinylated to prevent the formation of large multimer ligation products. Time course assays containing Ku, which is required for efficient blunt-end ligation (19), and X4-LIV revealed that the addition of a 5′-PO_4 to the unlabeled bottom strand does not stimulate ligation (Fig. 5, *lanes 6–10*). In fact, the presence of both 5′-PO_4 groups results in a lower ligation efficiency than does a 5′-PO_4 at only one of the two DNA ends (Fig. 5). The removal of the 3′-OH from the unlabeled bottom strand, however, results in a decrease in ligation of the top strand to almost undetectable levels (Fig. 6, *lanes 6–10*). This shows that both 3′-OH groups play a critical role in the ligation of two blunt DNA ends, whereas a second 5′-PO_4 is not necessary. Overall, these data demonstrate the effect of DNA end configuration on Artemis stimulation and blunt-end ligation by X4-LIV, unifying both of these related roles of X4-LIV in DNA end processing.

The XRCC4-DNA ligase IV complex interferes with Artemis·DNA-PKcs action at 3′ overhangs

We observed across all of the Artemis nuclease assays that the sum of all cleavage products (both 5′ and 3′) was greater for reactions containing the X4-LIV complex relative to those containing only Artemis and DNA-PKcs. To examine this in more detail, we quantitated 3′ and 5′ cutting efficiencies separately in the assays where these cleavage products are both generated (*i.e.* assays containing 3′ overhangs). We found that there are more 3′ than 5′ cleavage products generated in reactions containing Artemis and DNA-PKcs without X4-LIV. However, the

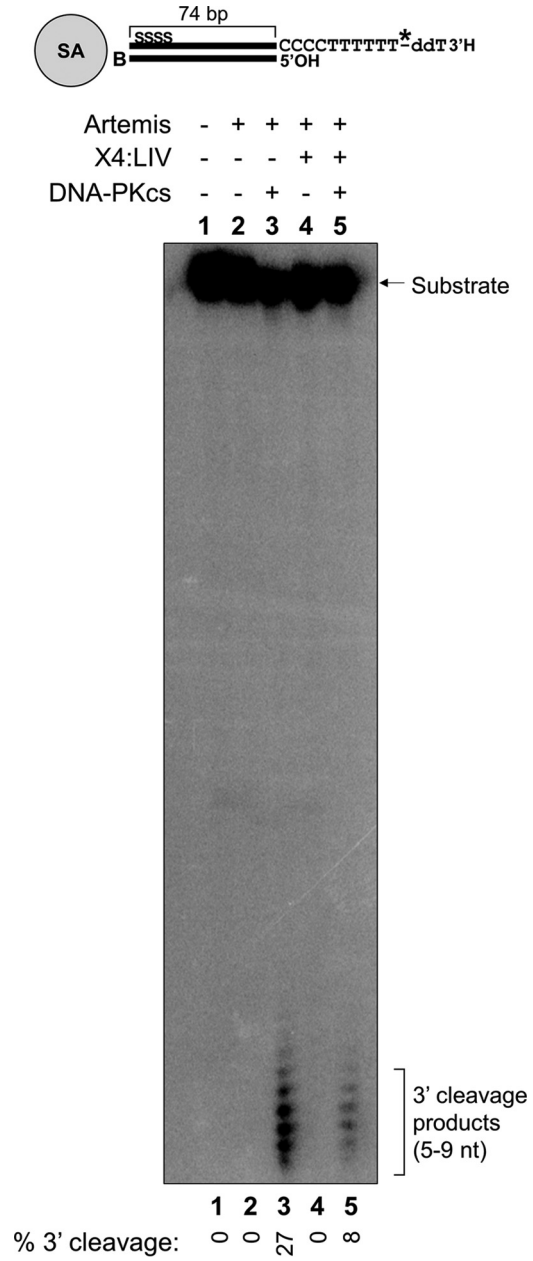

Figure 7. XRCC4-DNA ligase IV and Artemis·DNA-PKcs do not simultaneously occupy a 3′ overhang DNA end. 50 nM Artemis, 100 nM X4-LIV, and 25 nM DNA-PKcs were incubated with 40 nM HC101/HC102* at 37 °C for 60 min. DNA was incubated with 200 nM streptavidin prior to the addition of NHEJ proteins to suppress protein binding or enzyme action at the biotinylated DNA end. DNA was resolved using 12% denaturing PAGE. The *asterisk* indicates a ^{32}P radiolabel, *B* indicates biotin, *SA* indicates streptavidin, and *ddT* indicates a 2′,3′-dideoxythymidine. Cleavage efficiency was calculated by dividing the signal of cleavage products by the total signal in each lane. Efficiency values were normalized to background signal in the substrate-only lane. This figure is representative of three gels from very similar experiments.

addition of X4-LIV results in a decrease in 3′ products and an increase in 5′ products (Fig. 1, *lane 3 versus 5*). This observation is consistent for both 3′ overhang substrates (Figs. 1 and 4).

To confirm this, we radiolabeled the 3′ end of a 74-bp duplex containing a 10-nt 3′ overhang and incubated with proteins as previously described (Fig. 7). We found that Artemis and DNA-PKcs generate more 3′ cleavage products than do Artemis, DNA-PKcs, and X4-LIV combined. In this case, although X4-LIV would not recognize the terminal dideoxythymidine at the 3′ overhang and would therefore not stimulate Artemis action at this DNA end, the Artemis·DNA-PKcs contribution accounts for cutting in lanes containing Artemis, DNA-PKcs, and X4-LIV (Fig. 7, *lane 5*). These data indicate that there is some interference between X4-LIV and DNA-PKcs with respect to Artemis action at 3′ overhangs.

Discussion

Previously, we have observed that Artemis cuts DNA overhangs in the presence of X4-LIV and absence of DNA-PKcs (19). This finding challenged our current understanding of the necessity of DNA-PKcs acting in complex with Artemis to support endonuclease activity. Here, using *in vitro* nuclease assays, we find that X4-LIV alone is sufficient to stimulate Artemis endonuclease activity specifically at 3′ overhangs containing a terminal OH. Analysis of the X4-LIV complex reveals the importance of the 3′-OH, but not the 5′-PO_4 of the same DNA end, for joining of blunt ends. We surmise, then, that the 3′-OH is not only necessary for ligation but also serves as a critical contact point for X4-LIV, where it can recruit Artemis, which can then act locally in the absence of DNA-PKcs.

DNA end chemical configuration serves as a XRCC4-DNA ligase IV recognition element

Mammalian DNA ligases I, III, and IV share features conserved in all DNA and RNA ligases; the nucleotidyl transferase and oligonucleotide/oligosaccharide binding-fold domains comprise the core catalytic region. An additional N-terminal DNA-binding domain found in the three mammalian DNA ligases is required for ligation activity (21, 22). Analysis of the crystal structure of DNA ligase I suggests that a 3′-OH is important for proper alignment of DNA ends in a nicked substrate. Both binding sites for divalent metal ions are coordinated such that they may position the 5′-PO_4 for efficient nucleophilic attack by the 3′-OH (21).

Our finding that X4-LIV stimulation of Artemis occurs only at 3′ overhangs supports the role of the 3′-OH as a critical contact point for X4-LIV, as this effect depends upon the availability of a sterically accessible 3′-OH not present in 3′ terminal dideoxynucleotides, 5′ overhangs or hairpins (Fig. 8*A*). This is further substantiated by the decrease in ligation activity observed upon the removal of a 3′-OH, but not a 5′-PO_4, at one DNA end. The disparity between these results and recent single-molecule fluorescence resonance energy transfer data, which suggests that it is the 5′-PO_4 that serves as the critical recognition element (20), can be accounted for by differences in which chemical reaction steps are being measured. Although single-molecule fluorescence resonance energy transfer was utilized for the evaluation of bridging of complementary 4-nt 3′ overhangs, here we measure covalent ligation of blunt ends. It is possible that bridging of the overhangs, which are subject to transient annealing, requires both 5′-PO_4 groups for stabilization. In contrast, the 3′-OH may be more critical for catalytic activity by X4-LIV to occur. This suggests that the catalytic step is rate-limiting rather than the noncovalent bridging step.

Interestingly, we find that having a 5′-PO_4 at both DNA ends results in a reduction in ligation efficiency as compared with a

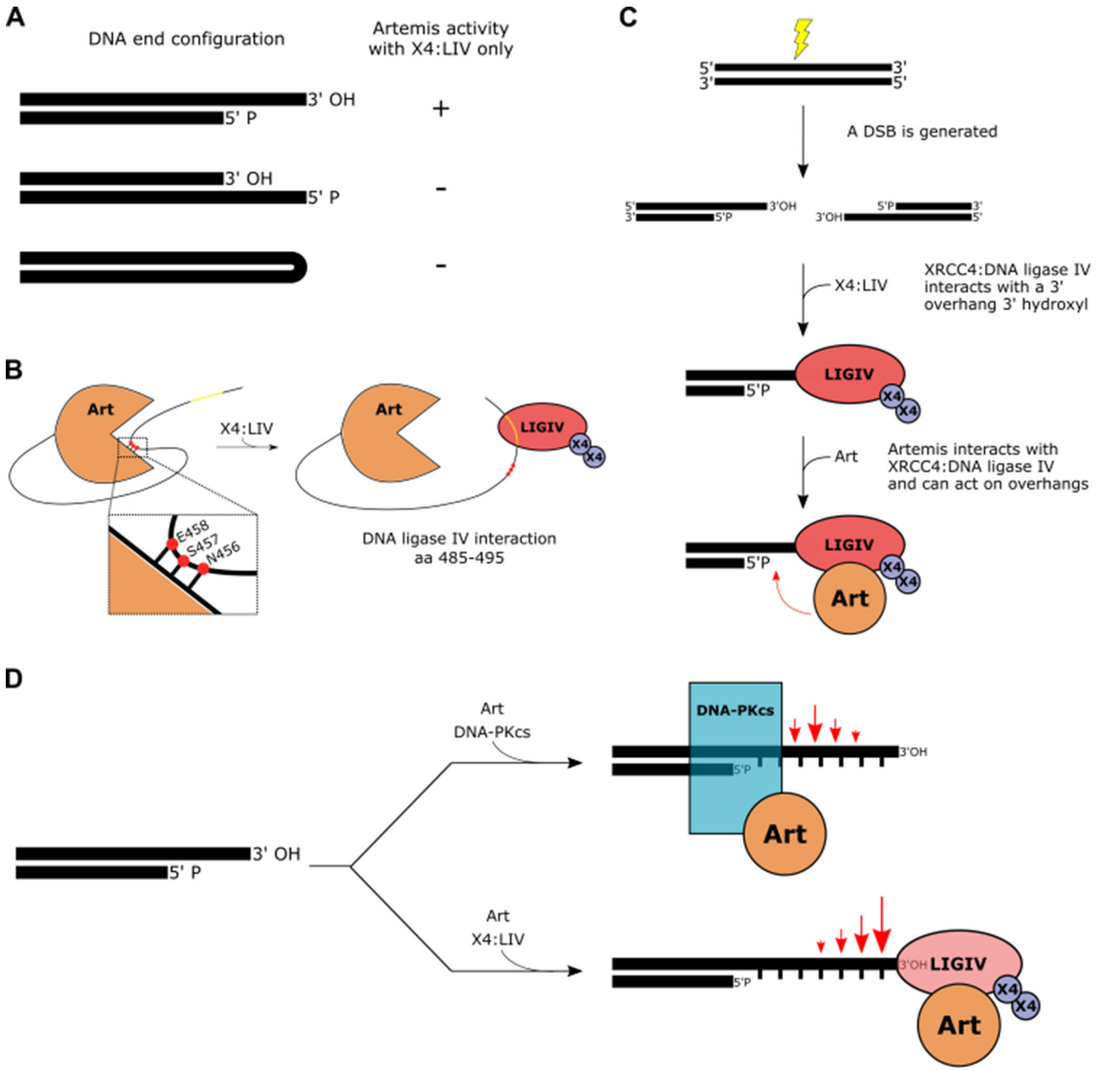

Figure 8. A model for stimulation of Artemis activity by XRCC4-DNA ligase IV. *A,* DNA-PKcs-independent Artemis activity, stimulated by X4-LIV, occurs specifically at 3′ overhangs containing a terminal 3′-hydroxyl group. *B*, Artemis is auto-inhibited by an interaction between its N-terminal catalytic domain and residues Asn-456, Ser-457, and Glu-458 (indicated by *red circles*) within its C-terminal tail (23). X4-LIV interacts with the DNA ligase IV interaction region of C-terminal Artemis at residues 485–495 (indicated in *yellow*) (24, 25). The interaction between X4-LIV and Artemis releases the autoinhibitory tail from the catalytic domain, allowing Artemis nuclease activity to occur. *C*, upon the generation of a DNA double-strand break, X4-LIV is recruited to a 3′ overhang DNA end through recognition of a terminal 3′-hydroxyl group. Artemis interacts with X4-LIV (described in *B*) and can act locally at 3′ overhangs. *D*, Artemis can process 3′ overhang DNA ends with either DNA-PKcs or X4-LIV. *Red arrows* indicate major and minor cut sites. The Artemis·DNA-PKcs complex preferentially cuts 4 nt 3′ of the ss/dsDNA boundary, with minor products generated near the major cut site. Artemis stimulated by X4-LIV acts locally, preferentially cutting 1 nt into the overhang end, with minor products generated 5′ of the major cut site, extending further into the overhang.

5′-PO_4 at only one end (Fig. 5). This result might be attributed to repulsion between the negatively charged 5′-PO_4 groups, making it less likely for the ends to be correctly aligned for ligation.

A model for XRCC4-DNA ligase IV stimulation of Artemis endonuclease activity

A recent study suggests a model of Artemis autoinhibition in which residues Asn-456, Ser-457, and Glu-458 within the C-terminal tail associate with the N-terminal catalytic region, preventing substrate binding and inhibiting nuclease activity (23). Artemis also contains a putative X4-LIV interaction domain at residues 485–495 within its C-terminal tail (24, 25). Consistent with our findings using full-length Artemis, a truncated Artemis mutant lacking a portion of the C-terminal tail is not stimulated for endonuclease activity at the 3′ overhang (data not shown). We propose that, after binding to a 3′ overhanging DNA strand via a 3′-OH recognition element, X4-LIV

recruits Artemis to the DNA end; the ligase complex may then activate Artemis by occupying the C-terminal X4-LIV-binding domain, thereby obstructing the interaction between the C-terminal tail residues and the N-terminal catalytic region (Fig. 8*B*). This model provides an explanation for targeting of Artemis to specific DNA end configurations as well as DNA-PKcs-independent endonuclease activity in the presence of X4-LIV specifically at 3′ overhang ends (Fig. 8*C*).

In addition to our finding that Artemis may be stimulated in the absence of DNA-PKcs, we also observe that X4-LIV stimulation of Artemis generates cleavage products closer to the 3′-OH. The Artemis·DNA-PKcs endonuclease preferentially cleaves 3′ overhangs 4–6 nt 3′ of the ss/dsDNA boundary (16). Here, we similarly find that the addition of DNA-PKcs results in cutting 3–6 nt 3′ of the ss/dsDNA boundary, with the major product at 4 nt (Fig. 8*D*). Interestingly, Artemis and X4-LIV (without DNA-PKcs) cut 1 nt 5′ of the 3′-OH, with minor products being generated as cutting extends further into the overhang (Fig. 8*D*). These observations are consistent with our model, where binding of X4-LIV at the 3′-OH directs Artemis to cut near that DNA end.

Physiological relevance of DNA-PKcs-independent Artemis endonuclease activity in V(D)J recombination

In wild-type pre-B or pre-T cells, during V(D)J recombination, each coding end typically suffers nucleolytic removal of 1 to 10 bp, contributing to the junctional diversification (26). The Artemis·DNA-PKcs complex is likely responsible for this action because this nuclease is already present at coding ends for hairpin opening. In wild-type pre-B or pre-T cells, the signal DNA ends only rarely suffer nucleotide loss (26).

In mutant mammalian cells lacking DNA-PKcs kinase activity (*e.g.* rodent mutants, such as murine SCID, or other SCID animals, such as equine SCID (27)), the signal ends often suffer more signal end nucleolytic processing than in wild-type cells (28, 29). There is substantial genetic and biochemical evidence indicating that Artemis is the nuclease responsible for this processing, even in the absence of DNA-PKcs (30). Some of this signal end processing may be due to the 5′ exonucleolytic action of Artemis, and this would leave a 3′ overhang. However, much of the signal end processing in these DNA-PKcs mutants extends further, and there has been no explanation for such deep nucleolytic processing (31). Our data here indicate that the endonucleolytic activity of Artemis could occur at these signal ends due to partial stimulation by the X4-LIV complex specifically at the 3′ overhangs generated by initial 5′ exonuclease action by Artemis. This type of activity would explain how processing by Artemis can extend so deeply into signal ends in mammalian pre-B and pre-T cells in the absence of DNA-PKcs.

In addition to explaining end processing during V(D)J recombination when DNA-PKcs is absent in mutant cells, our studies are also relevant to the coding end processing in wild-type pre-B and pre-T cells. Hairpin cleavage typically generates a 4-nt 3′ overhang with a terminal 3′-OH. These studies show that this configuration is suitable for further processing by Artemis upon stimulation by either DNA-PKcs or X4-LIV.

Physiological relevance of DNA-PKcs-independent Artemis endonuclease activity in NHEJ

When mammalian cells are subjected to ionizing radiation or chemical agents that cause DSBs, cells lacking DNA ligase IV are the most vulnerable. Cells lacking DNA-PKcs are sensitive, but not as sensitive as cells lacking DNA ligase IV (32). The results in our study show that Artemis is partially activated at a subset of DNA end configurations (3′ overhangs) through recognition of the 3′-OH by the X4-LIV complex and, therefore, is able to contribute to the endonucleolytic processing of a subset of DSBs even in the absence of DNA-PKcs.

Of relevance to the wild-type situation, when DNA-PKcs is not competing with X4-LIV at a 3′ overhang, Artemis has its highest potential for nuclease activity. The reduction in Artemis·DNA-PKcs cutting when X4-LIV is present at the 3′ overhang suggests that the ligase complex and this nuclease complex cannot occupy the same 3′ overhang at the same time. Such sequential action agrees with our biochemical reconstitution joining data (33) and our data from junctions formed within cells during V(D)J recombination (26).

Experimental procedures

Oligonucleotides and DNA substrates

Oligonucleotides used in this study were synthesized by Integrated DNA Technologies, Inc. (San Diego, CA). Oligonucleotides were purified using 8 or 12% denaturing PAGE and DNA concentration was determined spectrophotometrically. 5′ end radiolabeling of oligonucleotides was performed using [γ-^{32}P]ATP (3000 Ci/mol) (PerkinElmer Life Sciences) and T4 polynucleotide kinase (New England Biolabs). 3′ end radiolabeling was performed using [α-^{32}P] thymidine triphosphate (3000 Ci/mol) (PerkinElmer Life Sciences) and terminal deoxynucleotidyl transferase (Promega). Termination of the 3′ end-labeling reaction was achieved by adding a 13-fold excess of unlabeled 2′,3′-dideoxythymidine to [α-^{32}P]TTP. Unincorporated radioisotope was removed using Sephadex G-25 spin columns (Epoch Life Science). Duplex DNA substrates were created by adding a 20% excess of unlabeled oligonucleotide to the radiolabeled complementary strand. To ensure hybridization and to reduce secondary structure formation, all substrates were heated at 95 °C for 5 min and cooled at room temperature for 3 h, then at 4 °C overnight. Sequences of oligonucleotides used in this study are as follows: HC101, 5′-C*G*T* T*AA GTA TCT GCA TCT TAC TTG ATG GAG GAT CCT GTC ACG TGC TAG ACT ACT GGT CAA GCG CAT CGA GAA CCC CCC TTT TTT-3′; HC102, 5′-GGT TCT CGA TGC GCT TGA CCA GTA GTC TAG CAC GTG ACA GGA TCC TCC ATC AAG TAA GAT GCA GAT ACT TAA CG-biotin-3′; HC115, 5′-GAT GCC TCC AAG GTC GAC GAT GCA GAC ACT GAT ATA TGT ACA GAT TCG GTT GAT CAT AGC ACA ATG CCT GCT GAA CCC ACT ATC G-3′; HC120, 5′-biotin-CGA TAG TGG GTT CAG CAG GCA TTG TGC TAT GAT CAA CCG AAT CTG TAC ATA TAT CAG TGT CTG CAT CGT CGA CCT TGG AGG CAT C-3′; HC121, 5′-C*G*T* T*AA GTA TCT GCA TCT TAC TTG ATG GAG GAT CCT GTC ACG TGC TAG ACT ACT GGT CAA GCG CAT CGA GAA CC-3′; HC127, 5′-A*T*T* A*CT ACG GTA

GTA GCT ACG TAG CTA CTA CCG TAG TAA T-3′; HC128, 5′-biotin-CGA GCC CGA TCC GCT TGA CCA GTA GTC TAG CAC GTG ACG ATT GCA TCC GTC AAG TAA GAT GCA GAT ACT TAA C-3′; CG03, 5′-C*G*T* T*AA GTA TCT GCA TCT TAC TTG ATG GAG GAT CCT GTC ACG TGC TAG ACT ACT GGT CAA GCG CAT CGA GAA CCC CCC TTT TT-dideoxy-C-3′; CG04, 5′-biotin-CGA TAG TGG GTT CAG CAG GCA TTG TGC TAT GAT CAA CCG AAT CTG TAC ATA TAT CAG TGT CTG CAT CGT CGA CCT TGG AGG CAT-dideoxyC-3′; CG11, 5′-C*G*T* T*AA GTA TCT GCA TCT TAC TTG ATG GAG GAT CCT GTC ACG TGC TAG ACT ACT GGT CAA GCG CAT CGA GAA CCC CCC TTT TTT TTT T-3′; CG12, 5′-TTT TTT TTT TTT TTT TTT TTT TTT TTT TTT TTT TTT TTT TTT TTT TTT TTT TTT TTT TTT TTT CAT CGA GAA CCC CCC TTT TTT-3′; SL23, 5′-T*T*T*T* T*TT TTG CCA GCT GAC GCG CGT CAG CTG GC-3′; JG163, 5′-GTT AAG TAT CTG CAT CTT ACT TGA CGG ATG CAA TCG TCA CGT GCT AGA CTA CTG GTC AAG CGG ATC GGG CTC GAC C-3′; JG166, 5′-CGA GCC CGA TCC GCT TGA CCA GTA GTC TAG CAC GTG ACG ATT GCA TCC GTC AAG TAA GAT GCA GAT ACT TAA CAG G-3′; JG277, 5′-TTT TTT CCC CGT TAA GTA TCT GCA TCT TAC TTG ACG GAT GCA ATC GTC ACG TGC TAG ACT ACT GGT CAA GCG GAT CGG GCT CG-3′. Asterisks indicate phosphorothioate linkages.

Protein expression and purification

The X4-LIV complex was expressed and purified using a baculovirus expression system in High Five cells (ThermoFisher Scientific). XRCC4 and C-terminal His-tagged DNA ligase IV recombinant baculoviruses were a gift from Dr. Dale Ramsden (University of North Carolina School of Medicine, Chapel Hill, NC). High Five cells were co-infected with XRCC4 and DNA ligase IV baculoviruses at an equal multiplicity of infection. Harvested cells were resuspended in Ni-NTA binding buffer (50 mM NaH_2PO_4 (pH 7.8), 500 mM KCl, 0.1% Triton X-100, 20 mM imidazole (pH 7.8), 2 mM β-mercaptoethanol) supplemented with protease inhibitors, then sonicated and centrifuged. The supernatant was applied to Ni-NTA-agarose resin (Qiagen). X4-LIV was eluted with elution buffer (binding buffer with 500 mM imidazole). High-resolution purification was performed using two-step column chromatography with the ÄKTAexplorer system (GE Healthcare Life Sciences). Ni-NTA affinity-purified eluate was dialyzed against Mono Q buffer A (50 mM Tris-HCl (pH 7.5), 150 mM KCl, 10% glycerol, 0.05% Triton X-100, 1 mM DTT, 0.2 mM PMSF), loaded onto a Mono Q 5/50 GL anion exchange column (GE Healthcare Life Sciences), and eluted with a linear gradient to 30% Mono Q buffer B (Mono Q buffer A with 1 M KCl). Peak fractions were pooled, dialyzed against Mono S buffer A (50 mM Tris-HCl (pH 7.5), 50 mM NaCl, 10% glycerol, 1 mM EDTA, 1 mM DTT, 0.2 mM PMSF), loaded onto a Mono S 5/50 GL cation exchange column (GE Healthcare Life Sciences), and eluted with a linear gradient to 100% Mono S buffer B (Mono S buffer A with 750 mM NaCl). Peak fractions were stored at −80 °C. Purified X4-LIV was found to be active and to have no detectable nuclease contamination. Purification of Ku, DNA-PKcs, and Artemis was performed as previously described (16, 34–36). Briefly, the recombinant Ku70/80 complex was purified from High Five cells by Ni-NTA affinity, dsDNA (oligo) affinity, and anion exchange chromatography. Endogenous DNA-PKcs was purified from HeLa cells using a series of column chromatography steps including anion exchange, cation exchange, dsDNA (oligo) affinity, and size exclusion chromatography. Artemis was purified from Sf9 cells by Ni-NTA affinity and anion exchange chromatography. Ku, DNA-PKcs, and Artemis were found to have no detectable nuclease contamination.

Nuclease assay

In vitro nuclease assays were performed in a 10-μl reaction volume in NHEJ buffer (25 mM Tris-HCl (pH 8.0), 75 mM KCl, 10 mM $MgCl_2$, 1 mM DTT, 0.5 mM ATP, 10% PEG 8000, with 200 nM streptavidin when using biotinylated substrates). Biotinylated DNA was incubated with excess streptavidin prior to the addition of proteins for efficient blocking of biotinylated DNA ends. Reactions containing 40 nM ^{32}P-radiolabeled DNA substrate, 50 nM Artemis, 25 nM DNA-PKcs, and 100 nM X4-LIV were incubated at 37 °C for 60 min. Ladders were generated by incubating 80 nM ^{32}P-radiolabeled ssDNA with 0.4 milliunits/ml of snake venom phosphodiesterase 1 (Sigma) at 37 °C for 10 min. Reactions were terminated by heat inactivation at 95 °C for 10 min. DNA was extracted using phenol:chloroform, resolved using either 8 or 12% denaturing PAGE, and detected by autoradiography. Nucleolytic activity was quantitated using Quantity One 1-D analysis software (Bio-Rad).

Ligation assay

In vitro ligation time courses were performed in a 12-μl reaction volume in NHEJ buffer. Reactions containing 20 nM ^{32}P-radiolabeled DNA substrate, 20 nM unlabeled substrate, 50 nM Ku, and 100 nM X4-LIV were incubated at 37 °C and 2-μl aliquots were removed at the indicated time points. Markers were generated using the same conditions. Reactions were terminated by heat inactivation at 95 °C for 10 min. DNA was extracted and detected and ligation was quantitated as described above.

Author contributions—C. A. G. performed all of the experiments shown, but H. H. Y. C. performed early versions of some of the experiments. G. W. purified many preparations of the native human DNA-PKcs and helped C. A. G. purify several preparations of the X4-LIV. H. H. Y. C. purified other preparations of X4-LIV, Ku, and Artemis. M. R. L. supervised the work. C. A. G. and M. R. L. wrote the manuscript with input from H. H. Y. C. and G. W.

Acknowledgment—We thank Dr. Ray Mosteller (USC) for comments on the manuscript.

References

1. Lieber, M. R. (2010) The mechanism of double-strand DNA break repair by the nonhomologous DNA end-joining pathway. *Annu. Rev. Biochem.* **79,** 181–211
2. Lieber, M. R., and Karanjawala, Z. E. (2004) Ageing, repetitive genomes and DNA damage. *Nat. Rev. Mol. Cell Biol.* **5,** 69–75
3. Martin, G., Smith, A., Ketterer, D., Ogburn, C., and Disteche, C. (1985) Increased chromosomal aberrations in first metaphases of cells isolated from the kidneys of aged mice. *Isr. J. Med. Sci.* **21,** 296–301

4. Santivasi, W. L., and Xia, F. (2014) Ionizing radiation-induced DNA damage, response, and repair. *Antioxid. Redox Signal.* **21,** 251–259
5. Chance, B., Sies, H., and Boveris, A. (1979) Hydroperoxide metabolism in mammalian organs. *Physiol. Rev.* **59,** 527–605
6. Karanjawala, Z. E., Adachi, N., Irvine, R. A., Oh, E. K., Shibata, D., Schwarz, K., Hsieh, C. L., and Lieber, M. R. (2002) The embryonic lethality in DNA ligase IV-deficient mice is rescued by deletion of Ku: implications for unifying the heterogeneous phenotypes of NHEJ mutants. *DNA Repair* **1,** 1017–1026
7. Ashour, M. E., Atteya, R., and El-Khamisy, S. F. (2015) Topoisomerase-mediated chromosomal break repair: an emerging player in many games. *Nat. Rev. Cancer* **15,** 137–151
8. Mahowald, G. K., Baron, J. M., and Sleckman, B. P. (2008) Collateral damage from antigen receptor gene diversification. *Cell* **135,** 1009–1012
9. Renkawitz, J., Lademann, C. A., and Jentsch, S. (2014) Mechanisms and principles of homology search during recombination. *Nat. Rev. Mol. Cell Biol.* **15,** 369–383
10. Symington, L. S., and Gautier, J. (2011) Double-strand break end resection and repair pathway choice. *Annu. Rev. Genet.* **45,** 247–271
11. Griffith, A. J., Blier, P. R., Mimori, T., and Hardin, J. A. (1992) Ku polypeptides synthesized *in vitro* assemble into complexes which recognize ends of double-stranded DNA. *J. Biol. Chem.* **267,** 331–338
12. West, R. B., Yaneva, M., and Lieber, M. R. (1998) Productive and nonproductive complexes of Ku and DNA-dependent protein kinase at DNA termini. *Mol. Cell. Biol.* **18,** 5908–5920
13. Gu, J., and Lieber, M. R. (2008) Mechanistic flexibility as a conserved theme across 3 billion years of nonhomologous DNA end-joining. *Genes Dev.* **22,** 411–415
14. Li, S., Kanno, S., Watanabe, R., Ogiwara, H., Kohno, T., Watanabe, G., Yasui, A., and Lieber, M. R. (2011) Polynucleotide kinase and aprataxin-like forkhead-associated protein (PALF) acts as both a single-stranded DNA endonuclease and a single-stranded DNA 3′ exonuclease and can participate in DNA end joining in a biochemical system. *J. Biol. Chem.* **286,** 36368–36377
15. Li, S., Chang, H. H., Niewolik, D., Hedrick, M. P., Pinkerton, A. B., Hassig, C. A., Schwarz, K., and Lieber, M. R. (2014) Evidence that the DNA endonuclease ARTEMIS also has intrinsic 5′-exonuclease activity. *J. Biol. Chem.* **289,** 7825–7834
16. Ma, Y., Pannicke, U., Schwarz, K., and Lieber, M. R. (2002) Hairpin opening and overhang processing by an Artemis/DNA-dependent protein kinase complex in nonhomologous end joining and V(D)J recombination. *Cell* **108,** 781–794
17. Niewolik, D., Pannicke, U., Lu, H., Ma, Y., Wang, L. C., Kulesza, P., Zandi, E., Lieber, M. R., and Schwarz, K. (2006) DNA-PKcs dependence of Artemis endonucleolytic activity, differences between hairpins and 5′ or 3′ overhangs. *J. Biol. Chem.* **281,** 33900–33909
18. Gu, J., Li, S., Zhang, X., Wang, L. C., Niewolik, D., Schwarz, K., Legerski, R. J., Zandi, E., and Lieber, M. R. (2010) DNA-PKcs regulates a single-stranded DNA endonuclease activity of Artemis. *DNA Repair* **9,** 429–437
19. Chang, H. H., Watanabe, G., Gerodimos, C. A., Ochi, T., Blundell, T. L., Jackson, S. P., and Lieber, M. R. (2016) Different DNA end configurations dictate which NHEJ components are most important for joining efficiency. *J. Biol. Chem.* **291,** 24377–24389
20. Reid, D. A., Conlin, M. P., Yin, Y., Chang, H. H., Watanabe, G., Lieber, M. R., Ramsden, D. A., and Rothenberg, E. (2017) Bridging of double-stranded breaks by the nonhomologous end-joining ligation complex is modulated by DNA end chemistry. *Nucleic Acids Res.* **45,** 1872–1878
21. Pascal, J. M., O'Brien, P. J., Tomkinson, A. E., and Ellenberger, T. (2004) Human DNA ligase I completely encircles and partially unwinds nicked DNA. *Nature* **432,** 473–478
22. Ellenberger, T., and Tomkinson, A. E. (2008) Eukaryotic DNA ligases: structural and functional insights. *Annu. Rev. Biochem.* **77,** 313–338
23. Niewolik, D., Peter, I., Butscher, C., and Schwarz, K. (2017) Autoinhibition of the nuclease ARTEMIS is mediated by a physical interaction between its catalytic and C-terminal domains. *J. Biol. Chem.* **292,** 3351–3365
24. De Ioannes, P., Malu, S., Cortes, P., and Aggarwal, A. K. (2012) Structural basis of DNA ligase IV-Artemis interaction in nonhomologous end-joining. *Cell Rep.* **2,** 1505–1512
25. Malu, S., De Ioannes, P., Kozlov, M., Greene, M., Francis, D., Hanna, M., Pena, J., Escalante, C. R., Kurosawa, A., Erdjument-Bromage, H., Tempst, P., Adachi, N., Vezzoni, P., Villa, A., Aggarwal, A. K., and Cortes, P. (2012) Artemis C-terminal region facilitates V(D)J recombination through its interactions with DNA ligase IV and DNA-PKcs. *J. Exp. Med.* **209,** 955–963
26. Gauss, G. H., and Lieber, M. R. (1996) Mechanistic constraints on diversity in human V(D)J recombination. *Mol. Cell. Biol.* **16,** 258–269
27. Meek, K., Dang, V., and Lees-Miller, S. P. (2008) DNA-PK: the means to justify the ends?. *Adv. Immunol.* **99,** 33–58
28. Kulesza, P., and Lieber, M. R. (1998) DNA-PK is essential only for coding joint formation in V(D)J recombination. *Nucleic Acids Res.* **26,** 3944–3948
29. Lieber, M. R., Hesse, J. E., Mizuuchi, K., and Gellert, M. (1988) Lymphoid V(D)J recombination: nucleotide insertion at signal joints as well as coding joints. *Proc. Natl. Acad. Sci. U.S.A.* **85,** 8588–8592
30. Touvrey, C., Couedel, C., Soulas, P., Couderc, R., Jasin, M., de Villartay, J. P., Marche, P. N., Jouvin-Marche, E., and Candéias, S. M. (2008) Distinct effects of DNA-PKcs and Artemis inactivation on signal joint formation *in vivo*. *Mol. Immunol.* **45,** 3383–3391
31. Lieber, M. R., Hesse, J. E., Lewis, S., Bosma, G. C., Rosenberg, N., Mizuuchi, K., Bosma, M. J., and Gellert, M. (1988) The defect in murine severe combined immune deficiency: joining of signal sequences but not coding segments in V(D)J recombination. *Cell* **55,** 7–16
32. Rooney, S., Sekiguchi, J., Zhu, C., Cheng, H. L., Manis, J., Whitlow, S., DeVido, J., Foy, D., Chaudhuri, J., Lombard, D., and Alt, F. W. (2002) Leaky SCID phenotype associated with defective V(D)J coding end processing in Artemis-deficient mice. *Mol. Cell* **10,** 1379–1390
33. Ma, Y., Lu, H., Tippin, B., Goodman, M. F., Shimazaki, N., Koiwai, O., Hsieh, C.-L., Schwarz, K., and Lieber, M. R. (2004) A biochemically defined system for mammalian nonhomologous DNA end joining. *Mol. Cell* **16,** 701–713
34. Pannicke, U., Ma, Y., Hopfner, K. P., Niewolik, D., Lieber, M. R., and Schwarz, K. (2004) Functional and biochemical dissection of the structure-specific nuclease ARTEMIS. *EMBO J.* **23,** 1987–1997
35. Goodarzi, A. A., and Lees-Miller, S. P. (2004) Biochemical characterization of the ataxia-telangiectasia mutated (ATM) protein from human cells. *DNA Repair* **3,** 753–767
36. Chang, H. H., Watanabe, G., and Lieber, M. R. (2015) Unifying the DNA end-processing roles of the Artemis nuclease: Ku-dependent Artemis resection at blunt DNA ends. *J. Biol. Chem.* **290,** 24036–24050